

AperTO - Archivio Istituzionale Open Access dell'Università di Torino

### MCM41 functionalized with ethylenediaminetriacetic acid for ion-exchange chromatography

**This is the author's manuscript**

*Original Citation:*

MCM41 functionalized with ethylenediaminetriacetic acid for ion-exchange chromatography / Maria Concetta Bruzzone; Corrado Sarzanini; Anna Maria Torchia; Marta Teodoro; Flaviano Testa; Alessandro Virga; Barbara Onida. - In: JOURNAL OF MATERIALS CHEMISTRY. - ISSN 0959-9428. - 21:2(2011), pp. 369-376.

*Availability:*

This version is available <http://hdl.handle.net/2318/82315> since

*Published version:*

DOI:10.1039/C0JM02291H

*Terms of use:*

Open Access

Anyone can freely access the full text of works made available as "Open Access". Works made available under a Creative Commons license can be used according to the terms and conditions of said license. Use of all other works requires consent of the right holder (author or publisher) if not exempted from copyright protection by the applicable law.

(Article begins on next page)



# UNIVERSITÀ DEGLI STUDI DI TORINO

***This is an author version of the contribution published on:***

*Questa è la versione dell'autore dell'opera:*

*[J. Mater. Chem, 21,2011, DOI 10.1039/C0JM02291H, Paper]*

***The definitive version is available at:***

*La versione definitiva è disponibile alla URL:*

*[<http://pubs.rsc.org/en/content/articlelanding/2011/jm/c0jm02291h#!divAbstract>]*

**MCM41 functionalized with ethylenediaminetriacetic acid for ion-exchange chromatography**

Maria Concetta Bruzzoniti,<sup>1,\*</sup> Corrado Sarzanini,<sup>1</sup> Anna Maria Torchia,<sup>2</sup> Marta Teodoro,<sup>2</sup> Flaviano Testa,<sup>2</sup> Alessandro Virga,<sup>3</sup> Barbara Onida<sup>3,§</sup>

<sup>1</sup> Dipartimento di Chimica Analitica – Università degli Studi di Torino, Via P. Giuria 5, 10125 Torino

<sup>2</sup> Dipartimento di Ingegneria Chimica e dei Materiali - Università della Calabria, Via Pietro Bucci Cubo 44A 87030 Rende (CS)

<sup>3</sup> Dipartimento di Scienza dei Materiali e Ingegneria Chimica, Politecnico di Torino, Corso Duca degli Abruzzi 24, 10129 Torino, Italy. <sup>§</sup>CR-INSTM for Materials with Controlled Porosity, Italy.

**\* Corresponding author**

Maria Concetta Bruzzoniti, PhD  
Dipartimento di Chimica Analitica  
Università degli Studi di Torino  
Via P. Giuria 5, 10125 Torino (Italy)  
Ph.: +39 011 6707844  
Fax: +39 011 6707615  
E-mail: mariaconcetta.bruzzoniti@unito.it

## Abstract

Synthesis of ED3A-MCM41 hybrid material is reported. ED3A organic moiety is a ethylenediaminetriacetic group and functionalised mesoporous silica is obtained through a “one-pot” synthesis procedure, yielding –COOH groups available on the surface without any further modification. The product has been characterized using different techniques (XRD, N<sub>2</sub> sorption, SEM, DTG, XRF, FTIR).

Due to its chemical structure, ED3A-MCM41 has been tested for on-line chromatographic application in ion exchange of probe metal ions of environmental importance (Cd<sup>2+</sup>, Cu<sup>2+</sup> and Zn<sup>2+</sup>). In order to identify the mechanisms acting (cation-exchange and chelation) during the separation of metal ions on ED3A-MCM41, the retention behaviour with non-complexing (methanesulfonic acid), and complexing (oxalic and pyridine-2,6-dicarboxylic acids) eluents was investigated.

The study revealed that the chelation mechanism is dominant in the retention of Zn<sup>2+</sup> and Cu<sup>2+</sup>, while for Cd<sup>2+</sup> the cation-exchange mechanism is prevailing. The different mechanisms acting on the retention of the three metal ions allowed optimizing a gradient for their separation. The chelating properties of the ED3A-MCM41 phase suggests its use for the analysis and preconcentration (and/or removal) of metal ions in highly saline matrix (synthetic seawater). Examples of separations of metal ions in this matrix are shown.

## 1. Introduction

Mesoporous silica-based materials show extremely interesting properties when provided with organic functions that modify the physico-chemical properties of the surface. These properties are enhanced from the very high internal surface and the acceptable stability in a quite wide range of pH typical of these materials.

The organic group can be linked after synthesis (post-synthesis grafting) or during the preparation of the material (one-pot or co-condensation method). Advantages and disadvantages of both methods have been extensively described.<sup>1</sup> However, the co-condensation method is preferred especially because of the compositional homogeneity of the product. The precursor used is generally a trialkoxysilane (OR)<sub>3</sub>-Si-R' where R is methyl or ethyl group and R' is an organic fragment. This fragment is alkyl, aryl, or a functional group.

A tremendous number of papers reports a variety of silylated organic functions which have been covalently linked to the silica surface using the two different techniques. The obtained organic-inorganic hybrid materials can be used in different technological fields. Surface chemistry is modified in terms of hydrophilic/hydrophobic properties and of reactivity with respect to chemical species that diffuse in the porous system.

In order to confer ions removal properties mesoporous materials functionalized with amino, carboxylic and thio groups have been prepared. Their properties have been extensively studied in the last years. They have been investigated for the removal of metal ions in the treatment of wastewater, in analytical methods such as preconcentration or as stationary phase in ionic HPLC columns.<sup>2,3</sup> Mesoporous silica particles have been modified with 2-thiophene-carbaldehyde for separation and preconcentration of palladium (II)<sup>4</sup> and salicylaldehyde for uranium (VI)<sup>5</sup>. Silver nanoparticles have been confined in SBA-15 mesoporous silica and used as a sensor for H<sub>2</sub>O<sub>2</sub> detection.<sup>6</sup> Porous sulfonic acid functionalized silica spheres, prepared by oxidation of thiol-functionalized mesoporous silica samples, obtained by co-condensation of mercaptopropyl)trimethoxysilane and tetraethoxysilane in the presence of cetyltrimethylammonium, were studied in order to evaluate their ion exchange behaviour and the cation exchange capacities against Na<sup>+</sup>, K<sup>+</sup>, Cu<sup>2+</sup>, and Ca<sup>2+</sup> were determined by batch experiments.<sup>7</sup>

Nanoporous organo-silicas have been synthesized using an imprinting method, with benzene- and diethylbenzene bridged polysilsesquioxane as precursors, for preconcentration and detection of trinitrotoluene adsorbed from soils.<sup>8</sup> Using similar strategies organo-silicas particles provided of chiral organo groups have been prepared and successfully tested for determining the enantiomeric purity of organo-silicas solids.<sup>9</sup>

The interest of researchers in mesoporous materials for adsorption of analytes from gas and liquid phase is continuously growing. The adsorption properties of different MCM-41 without and with functional groups have been studied by inverse gas chromatography.<sup>10</sup> The surface polarity depends on the presence of functional group and induces the typical chromatographic behaviour where less-polar probes are eluted before polar ones. MCM-41 silica materials as such<sup>11,12</sup> or modified with aluminum<sup>13</sup> or -NH<sub>2</sub> and -SH groups<sup>14</sup> have been extensively studied for the adsorption of metal ions. Some applications of MCM-41 materials modified with C<sub>4</sub><sup>15</sup> or C<sub>8</sub><sup>15,16</sup> alkyl chains shows great potentiality for organic compounds separation.

Different methods for the preparation of silica spheres as materials for the packing of HPLC columns have been reported.<sup>17</sup> Hierarchical monolith silica with MSU-type mesoporous structure has been prepared through direct synthesis.<sup>18</sup> The authors claim that this material with bimodal porosity is effective in separation of benzene and phenol and it is promising as stationary phase in high performance liquid chromatography. For HPLC application it is also important a precise control of the morphology and of the particle size of the mesoporous material. A new type of surfactant, named Jeffamine, allows to obtain silica particles with pore size up to 200 Å and particle size between 1 and 1.7 μm.<sup>19</sup> In a similar paper particle size between 1 and 2 μm and good size distribution have been synthesized by a careful control of synthesis conditions with ammonia

catalysed hydrolysis. The pore size was successively expanded by a post-synthesis hydrothermal treatment.<sup>20</sup>

Within this frame, aim of this work is to prepare, to characterize and to test a silica-based mesoporous material provided with an organic multifunctional moiety able to work in chromatographic application. The precursor chosen for the covalent incorporation in MCM-41 yields an ethylenediaminetriacetic acid, ED3A, function on the surface, which potentially allows for multiple metal-ligand interactions. The only example of mesoporous silica functionalized with ethylenediaminetriacetic acid groups so far reported concerns modified SBA-15, which was used for the selective adsorption of  $\text{Cu}^{2+}$ .<sup>21</sup>

The performance of MCM-41 modified with ED3A (ED3A-MCM41) was here evaluated for on-line chromatographic applications. Due to ion-exchange and chelating properties expected, selected transition metal ions, namely  $\text{Cd}^{2+}$ ,  $\text{Cu}^{2+}$  and  $\text{Zn}^{2+}$ , has been chosen. The mechanisms acting during the elution process have been elucidated.

To the best of our knowledge this is the first application of chelating mesoporous material as a support in ion chromatography. In addition, the carboxylic groups are incorporated as-such during the synthesis of the mesoporous material and not obtained after hydrolysis of the  $-\text{CN}$  group as already reported.<sup>22</sup> Synthesis has been carried out using a S<sup>+</sup>I assembly of a cetyltrimethylammonium surfactant S<sup>+</sup> and an adequate mixture of tetraethylorthosilicate and sodium N-(trimethoxysilylpropyl)ethylenediaminetriacetate as organo-silica framework precursors.

## 2. Experimental

### 2.1 Chemicals

The hexadecyltrimethylammonium bromide (CTMABr) and tetraethylorthosilicate (TEOS, 98%) were from Aldrich (Milwaukee, MI, USA).  $(\text{MeO})_3\text{Si}(\text{CH}_2)_3\text{N}(\text{CH}_2\text{COONa})(\text{CH}_2)_2\text{N}(\text{CH}_2\text{COONa})_2$  was from Gelest (Morrisville, PA, USA). Ethanol (98 %),  $\text{NH}_4\text{OH}$  (30%) and  $\text{HCl}$  (37%) were from Carlo Erba (Milan, Italy).

Deionized water (18.2 M $\Omega$  cm resistivity at 25 °C ) from a water purification system (Milli Q Academic, Millipore) was used for the preparation of the eluents and standards. Stock solutions (1000 mgL<sup>-1</sup>) of  $\text{Cd}^{2+}$ ,  $\text{Cu}^{2+}$ ,  $\text{Zn}^{2+}$  prepared from Titrisol standard solutions (Merck) were properly diluted at the concentrations desired. Methanesulfonic acid (MSA) 70% in water, was from Aldrich, methanol (HPLC grade), pyridine-2,6-dicarboxylic acid (PDCA) was from Fluka and sodium nitrate was from J.T. Baker. Prior to use, all eluents were filtered through a 0.22  $\mu\text{m}$  filter. Analytes were injected at 5 mgL<sup>-1</sup>.

## 2.2 Equipment

The X-ray diffractometer was a Philips PW 1710 (CuK $\alpha$  radiation). Nitrogen adsorption-desorption measurements were conducted with a Micromeritics ASAP2010 sorptometer. Before the analysis the sample was outgassed at 150 °C for 12 hours.

TGA analysis was performed by a STA429 instrument (Netzsch GmbH, Selb, Germany).

X-Ray fluorescence analysis was performed with a Rigaku ZSX instrument.

For FTIR measurements the powder was pressed into a thin self-supporting wafer, which was placed into a quartz IR cell then connected to a vacuum frame and outgassed (residual pressure < 10<sup>-3</sup> mbar) at the desired temperature (from room temperature up to 150 °C). Spectra were recorded using a Bruker Equinox 55 spectrometer operating at 2 cm<sup>-1</sup> resolution. Dosage of ammonia (from Messer) was carried out at room temperature.

Chromatographic separations have been performed by a 4000i ion chromatograph (Dionex, Sunnyvale, CA, USA) equipped with a Rheodyne injector Model 7125 (sample loop 100  $\mu$ L) and with a VDM-II variable-wavelength UV-Vis detector. Eluent flow rate has been set at 0.3 mL min<sup>-1</sup>. Spectrophotometric detection has been performed at 520 nm after a post-column reaction with 0.4 mM 4-(2-pyridylazo)-resorcinol (PAR) in 0.3 M NaHCO<sub>3</sub>, 1 M 2-dimethylaminoethanol, 0.5 M NH<sub>4</sub>OH.

## 2.3 Material synthesis

In this preparation 1.44 g TEOS, 0.65 g sodium N-(trimethoxysilylpropyl)ethylenediaminetriacetate (ED3A silane) and 3.05 g ethanol have been added and kept under magnetic stirring for about 5 minutes in a flask (solution A). At the same time, 1.15 g CTMABr have been dissolved in 24.23 g of ultrapure water together with 6.30 g NH<sub>4</sub>OH and 20 g of ethanol (solution B). After complete dissolution, solution B has been mixed with solution A and the resulting mixture has been kept under mild magnetic stirring at room temperature for 2 hours. The resulting molar composition of the final ED3A-MCM41 material is the following:

TEOS:ED3A silane:CTMABr:NH<sub>4</sub>OH:EtOH:H<sub>2</sub>O=0.70:0.30:0.41:7:65:175.

Finally, the synthesis product has been recovered, filtered, washed with ultrapure water and dried at room temperature.

Surfactant has been removed through solvent extraction. In particular, 1.5 g of dried material have been dispersed in 500 ml of ethanol acidified with 10 ml of 5M HCl and kept under magnetic

stirring in an ultrasound bath at 60 °C for 6 hours. For the same material the procedure has been repeated two times. A pictorial scheme of the ED3A-MCM41 material is given in Figure 1.

#### *2.4 Column packing*

A PolyEtherEtherKethone (PEEK) column (50 mm x 4 mm i.d.) has been slurry packed<sup>2,3</sup> with about 0.5 g ED3A-MCM41 in 50 mL CH<sub>3</sub>OH by a Minipuls 3 peristaltic pump (Gilson Inc., Middleton, WI, USA) set at 13 rpm. The column was subsequently equilibrated with H<sub>2</sub>O at 0.5 mL/min under high pressure by connecting a peek tube of 2.6 mm with an internal diameter of 0.08 mm (0.003 inches, 1 µl/ft volume), generating a backpressure of about 2850 psi/m at 1 mL/min (Dionex Co., Sunnyvale, USA). The slurry packing and the equilibration was continued until the column was completely filled. The operating back-pressure of the column at 0.3 mL/min ranged between 1700 and 1800 psi. The void volume of the column, evaluated as the water deep in the chromatogram, was 0.6 mL.

#### *2.5 Column washing protocol and column performance*

For each experiment, before changing the eluent composition, and after each day of measurements the column was washed with 25 mL of 2.5 mM PDCA (Merck) at 0.3 mL/min. The re-equilibration of the column was performed with at least 18 mL eluent solution at 0.3 mL/min until a stable baseline was obtained. This procedure ensured a good within-day (RSD%= 0.7) and between-day (RSD%= 1.5) repeatability of retention times for  $t_r$  as long as about 17 min.

### **3 Results and discussion**

#### *3.1 Structure characterization*

X-Ray diffraction pattern of the sample after surfactant extraction is shown in Figure 2. It is characterized by a sharp (100) reflection at 2.25 2 $\theta$  degree and higher reflections at 3.95 2 $\theta$  (110) and 4.60 2 $\theta$  (200) denoting a good long-range order of the hexagonal structure which is not compromised by the presence of the organosilane molecule. In Figure 3 nitrogen adsorption-desorption isotherms at 77 K are reported. The adsorption is reversible and the isotherms are of Type 4. BET Specific Surface Area results ca. 1200 m<sup>2</sup>/g while the pore diameter calculated with the BJH method in the desorption branch is about 20 Å.

SEM micrograph of ED3A-MCM41 (available as Electronic Supplementary Information) shows spherical particles having size smaller than 1 µm.

Thermogravimetric analysis (not reported) has been carried out to evaluate the amount of ED3A in the mesoporous material. The observed weight loss between 200 and 550 °C was assigned to the



decomposition of the organic molecules, giving a content of 0.66 mmoles of ED3A per gram of SiO<sub>2</sub>. This value is obtained considering the three carboxylic group in their protonic form. Indeed, XR-fluorescence analysis (not reported) did not reveal the presence of residual Na<sup>+</sup> ions.

The IR spectrum of extracted ED3A-MCM41 after outgassing at room temperature is shown in Figure 4.

In the high frequency region an intense, broad and composite absorption is observed, centred at 3390 cm<sup>-1</sup>, which is due the H-bonded hydroxyls, i.e. Si-OH, -CO-OH and H<sub>2</sub>O. A weak shoulder due to non H-bonded silanols is discernable at 3738 cm<sup>-1</sup>.

The weak bands in the range 2800-3000 cm<sup>-1</sup> superimposed to the broad absorption are due to -CH<sub>2</sub>- stretching modes of the ED3A moieties.

In the low frequencies region (reported in detail in the inset), the band at 1724 cm<sup>-1</sup> is due to the C=O stretching mode of carboxylic groups in the ED3A moieties. Its frequency is significantly lower than that observed for free carboxylic groups (for instance 1780 cm<sup>-1</sup> for the butanoic acid in gas phase): this strongly suggests that -COOH species are engaged each in two H-bonding interactions, *i.e.* one as proton-acceptor at the carbonyl oxygen atom, and the other as proton-donor at the hydroxyl group.<sup>23</sup> In the same region, the band due to the -O-H bending mode is observed at 1380 cm<sup>-1</sup> (asterisk in the inset).<sup>24</sup>

An intense band is observed at 1634 cm<sup>-1</sup>, and it is ascribed to the bending mode of adsorbed molecular water. The presence of a large amount of adsorbed molecular water after outgassing at room temperature has not been observed for MCM-41 as such (spectrum not reported), neither for SBA-15 mesoporous silicas modified with carboxylic groups.<sup>2</sup> We tentatively ascribe the band at 1634 cm<sup>-1</sup> to water molecules interacting with couples of -COOH groups in the ED3A moieties, where two carboxylic groups act as ligands and coordinate one H<sub>2</sub>O molecule (or small water clusters). This coordination may account for the presence of water molecules strongly retained on the surface. Indeed, this band is intense also in the spectrum recorded after outgassing at 100 °C (Figure 5).

At lower frequency a shoulder is discernible at 1580 cm<sup>-1</sup>, which is ascribed, together with the weak band at 1400 cm<sup>-1</sup> (arrows in the figure), to the stretching modes of -COO<sup>-</sup> species,<sup>25</sup> formed by dissociation of carboxylic groups. The counteranions are likely to be hydronium ions, obtained by the proton transfer from the -COOH groups to molecular water. The stretching mode and the bending mode<sup>26</sup> of H<sub>3</sub>O<sup>+</sup> are most probably hidden in the broad absorption of the H-bonded -OH species and in the C=O stretching mode, respectively. This interpretation is supported by the evidence that the outgassing at 100 °C (broken curve in Figure 6), which causes partial removal of adsorbed water, yields the decrease of the shoulder at 1580 cm<sup>-1</sup> and the band at 1400 cm<sup>-1</sup>, due to

dissociated  $\text{-COO}^-$  species, accompanied by the increase of the  $\text{C=O}$  stretching mode of  $\text{-COOH}$  species at  $1730\text{ cm}^{-1}$ .

The weak bands at  $1467\text{ cm}^{-1}$  and  $1450\text{ cm}^{-1}$  are assigned to  $\text{-CH}_2\text{-}$  bending modes of the ED3A moieties.

The accessibility of carboxylic groups, which is prerequisite for their retention activity towards metal ions, has been investigated by means of ammonia adsorption at room temperature.

Figure 6 reports the spectra related to the sample outgassed at  $150\text{ }^\circ\text{C}$  in contact with ammonia at increasing equilibrium pressure.

Upon interaction with ammonia bands increase at  $1580\text{ cm}^{-1}$ , at  $1460\text{ cm}^{-1}$  (superimposed to the  $\text{-CH}_2\text{-}$  bending modes) and at  $1403\text{ cm}^{-1}$ .

The couple of bands at  $1580\text{ cm}^{-1}$  and  $1403\text{ cm}^{-1}$  is due to the stretching modes of  $\text{-COO}^-$  carboxylate species, whereas the band at  $1460\text{ cm}^{-1}$  is due to the bending mode of ammonium ion: these species are formed by proton transfer from  $\text{-COOH}$  groups to  $\text{NH}_3$  molecules. Indeed in same spectra bands due to  $\text{-COOH}$  species at  $1730\text{ cm}^{-1}$  and  $1380\text{ cm}^{-1}$  decrease. The spectroscopic evidence shows that carboxylic groups are accessible and reactive towards gaseous ammonia.

### 3.2 Chromatographic application of ED3A-MCM41

The ethylenediaminetriacetic functional group present in the ED3A-MCM41 sample can be exploited for the retention of transition metal ions in chromatographic applications; therefore, a PEEK column was slurry packed as described in section 2.4 and used as analytical column for the elution of  $\text{Cd}^{2+}$ ,  $\text{Cu}^{2+}$  and  $\text{Zn}^{2+}$ .

Mainly two interactions can be involved in the retention mechanism, namely: (i) the chelation of metal ions *via* the iminoacetic functionality, and/or (ii) the cation-exchange between metal ions and the carboxylic groups.

Considering the expected interactions, two different eluents have been tested: methanesulfonic acid (MSA) and pyridine-2,6-dicarboxylic acid (PDCA).

MSA is the eluent usually employed for cation-exchange separations.<sup>27</sup> The  $\text{H}^+$  ions from MSA displace the cations electrostatically interacting with the ED3A-MCM41 phase according to eq. (1)



(1)

If chelation interactions are expected, a ligand-assisted separation can be performed if a proper ligand is added in the eluent phase.

### 3.2.1 Effect of MSA on the retention behaviour

To evaluate the chromatographic behaviour of ED3A-MCM41 as stationary phase for metal ions, MSA has been initially used (3.5-15 mM).

Interestingly, a MSA based eluent elutes only  $\text{Cd}^{2+}$  (Figure 7), whilst the other cations are not eluted, meaning that interactions other than electrostatic must be expected, mainly chelation. The  $k$  data for  $\text{Cd}^{2+}$  fitted to the ion-exchange mechanism equation: <sup>28</sup>

$$\log k = a - x/y \log[\text{H}^+] \quad (2)$$

where  $x$  is the charge of the analyte ion,  $y$  is the charge of  $\text{H}^+$ , and  $a$  is a constant, provided a slope of 2.1 ( $r^2=0.955$ ), which is in good agreement with the theoretical charge.

### 3.2.2 Effect of ionic strength ( $I$ ) on the retention behaviour

It is well known that any ion-exchange interaction can be minimised through the use of high ionic strength eluents <sup>29</sup> with alkali metals salts generally used to increase  $I$ . In fact, with chelation mechanism, the alkali metals form such extremely weak coordinate bonds that they can be neglected in comparison to the polyvalent metal ion coordinate bond. Consequently, the effect of alkali metal concentration will be small.

Experiments were performed keeping constant MSA concentration (3.5 mM) and evaluating the effect of ionic strength (10-800 mM  $\text{NaNO}_3$ , Figure 8). Note that  $\text{Cd}^{2+}$  is still the only analyte eluted, confirming its retention on the phase by a cation-exchange mechanism and confirming also that  $\text{Zn}^{2+}$  and  $\text{Cu}^{2+}$  are instead retained by a chelation mechanism. Nevertheless, since increasing  $\text{NaNO}_3$  concentration from 400 to 800 mM  $\text{Cd}^{2+}$  reduce the retention time only by 1.5 min and since retention factor does not approach to zero (i.e.:  $t_r \neq t_0$ ) a chelating contribution during retention must be assumed also for  $\text{Cd}^{2+}$ .

### 3.2.3 Effect of ligands on the retention behaviour

For chelation chromatography, the presence of a complexing agent in the mobile phase will introduce a competitive effect for the analyte with the chelating group on the surface of the substrate; so all analytes are expected to be eluted. Pyridine-2,6-dicarboxylic (PDCA) and oxalic acid are ligands with different complexation characteristics (table 1) and were chosen as ligands.

#### 3.2.3.1 PDCA

If we assume that the chelating moiety in the stationary phase can be assimilated to the N-(2-Hydroxyethyl)ethylenediamine-N, N', N'-triacetic acid (HEDTA), PDCA can compete with the

chelating group of the stationary phase for the complexation of metal ions (see formation constants with the analytes in Table 1).

The effect of PDCA concentration was tested at constant pH value (pH 2) on the retention of the metal ions and the results obtained are shown in Figure 9. It is possible to note that PDCA does elute also  $\text{Cu}^{2+}$  and  $\text{Zn}^{2+}$  previously retained (an overlay of typical chromatograms obtained is shown in the inset of Figure 9), thus confirming the chelation properties of the ED3A-MCM41 phase and the competitive effect of PDCA.

In the presence of PDCA, if compared with the non-complexing MSA eluent at the same pH conditions (pH 2.0),  $\text{Cd}^{2+}$  reduces its retention ( $k_{\text{MSA}}=1.3$  vs  $k_{\text{PDCA}}=0.4$ ), meaning that it is complexed by PDCA thus supporting a mixed retention mechanism (chelation-cation-exchange). The obtained data support the hypothesis that  $\text{Cu}^{2+}$  and  $\text{Zn}^{2+}$  are instead retained mainly by chelation.

In order to get a better comprehension of the interactions between the ED3A-MCM41 phase and the metal ions, the effect of pH, for a PDCA containing eluent, on retention times has also been considered and results are plotted in Figure 10. These conditions allow us to evaluate the contributions of both mobile and ED3A-MCM41 phases to retention. For the equilibria ED3A-MCM41 phase, retention through both complexation and mainly cation-exchange mechanisms should be favoured due to the dissociation of the carboxylic groups so leading to higher retention times with the increase of pH. For the equilibria in the mobile phase, under a chelation retention mechanism, the increase of pH leads to stronger competition of PDCA, due to the increased concentration of its dissociated form ( $\text{p}K_1 = 2$ ,  $\text{p}K_2 = 4.5$ ) and retention times are expected to decrease. Under a cation-exchange mechanism, higher pH values, i.e. lower  $\text{H}^+$  concentration, lead to higher retention times. This is schematically depicted in the inset of Figure 10.

The chromatographic behaviour of  $\text{Cu}^{2+}$  and  $\text{Zn}^{2+}$  is in agreement mainly with the chelation mechanism. Retention for  $\text{Cd}^{2+}$  keeps constant since minimum already at pH 2, meaning that the interaction with PDCA prevails over other equilibria.

### 3.1.3.2 Oxalic acid

Oxalic acid is a mildly acidic complexing agent that is usually employed for the IC separation of transition metal ions. In order to accomplish elution and separation of metal ions, oxalic acid has been tested at different concentrations and pH values according to Table 2. It is possible to see that only oxalic acid concentration as high as 20 mM (pH 1.8) can achieve the elution of all analytes.

A mobile phase at the same ligand concentration, 20 mM oxalic acid, but pH 4.0 by addition of NaOH does not provide the elution of the analytes. This is in agreement with strong interactions (chelation or cation-exchange, see Figure 10 mechanisms) with the ED3A-MCM41 phase. The comparison of these experiments with those ones carried out at pH 1.8 by MSA (Figure 7) under non-complexing eluent conditions allows identifying the interactions involved. Results indicate that since  $k_{Cd}$  (pH 1.8, MSA)= 0.3 and  $k_{Cd}$  (pH 1.8, oxalic acid)= 0.04 for  $Cd^{2+}$  a prevail of the cation-exchange mechanism must be assumed together with a contribution of chelation in the stationary phase. On the other hand, chelation in the stationary phase must be assumed for  $Cu^{2+}$  and  $Zn^{2+}$ . This was also confirmed by running experiments at 20 mM oxalic acid, pH 1.8 and increasing  $I$  from 0 up to 75 mM  $NaNO_3$ . Under a cation-exchange mechanism, the addition of a counter-cation should decrease the retention of analyte species. Nevertheless, if an additional mechanism, i.e. complexation/chelation, is contributing to the retention, it is expected that the effect of eluent strength upon retention will be minor than that observed if simple cation-exchange were the only retention mechanism.<sup>30</sup> Since  $k_{Cu}$  values changes only slightly from 13.5 to 9.0 in the whole range investigated and  $k_{Zn}$  values remain almost unchanged, it can be confirmed that the chelation mechanism is acting on their retention. It should be stressed that the retention order obtained with oxalic acid in the eluent ( $Cd^{2+} < Zn^{2+} < Cu^{2+}$ ) is different from what obtained by PDCA eluent ( $Cd^{2+} < Cu^{2+} < Zn^{2+}$ ). This fact reflects the affinity order with the functional chelating group in the ED3A-MCM41 phase. The change of the selectivity obtained allows the separation between  $Zn^{2+}$  and  $Cu^{2+}$ , previously coeluted.

#### 3.2.4 Optimization of the separation

To summarize, PDCA accomplished the elution of all the analytes with the coelution of  $Zn^{2+}$  and  $Cu^{2+}$ ; instead, oxalic acid enabled the separation of  $Zn^{2+}$  and  $Cu^{2+}$ , but with long analysis time.

To attempt a separation, both the ligands were added in the eluent. In such a way we expect that  $Cu^{2+}$  and  $Zn^{2+}$  can be separated by the effect of oxalic acid while at the same time PDCA can anticipate the elution of  $Cu^{2+}$ . Figure 11a shows the separation of the mixture obtained at 2.5 mM PDCA, 20 mM oxalic acid, pH 1.8. An incomplete resolution between  $Zn^{2+}$  and  $Cu^{2+}$  peaks is still observed due to the effect of PDCA in the mobile phase. The partial coelution was faced through the use of a gradient which included a conditioning step without PDCA to enhance the separation of  $Cu^{2+}$  and  $Zn^{2+}$  (20 mM Oxalic acid, 50 mM  $NaNO_3$ , pH 1.8) and a step change at 3 min to 2.5 mM PDCA, 50 mM  $NaNO_3$ , pH 2.8 to obtain the elution of  $Cu^{2+}$  at reasonable retention times. The optimized separation is shown in Figure 11b.

### 3.2.5. Applications: synthetic sea water analysis

It was demonstrated that a chelation mechanism is acting in the retention of the metal ions considered. This behaviour is particularly enhanced for  $Zn^{2+}$  and  $Cu^{2+}$ . Under this property of the ED3A-MCM41 phase, the column was tested for the separation of the metal ions in a highly salinity matrix (i.e.: 0.5 M NaCl, synthetic sea water). The high amount of  $Na^+$  strongly interferes in the classical separation by cation-exchange and prevents the analysis of samples of environmental importance. Nevertheless, in this instance, the low affinity of  $Na^+$  ion for chelation groups, allow the analysis of this matrix without any interference. In Figure 12 the chromatograms of 0.5 M NaCl and 0.5 M NaCl spiked with 2.5 ppm of each metal ion are shown, where is possible to observe that no interference is given by the matrix.

## Conclusions

MCM-41 functionalized with ethylenediaminetriacetic acid (ED3A) by means of a one-step co-condensation procedure has been prepared and characterized. The presence of the organic precursor sodium N-trimethoxysilylpropyl)ethylenediaminetriacetate in the synthesis batch does not prevent the formation of an ordered hexagonal mesostructure. Surface carboxylic groups have been incorporated as-such and not obtained by hydrolysis of  $-CN$  groups, as usually reported. They are shown by IR characterization to be accessible and reactive towards gaseous ammonia.

For the first time a mesoporous silica functionalized with ED3A has been used in ion-exchange chromatographic application. The contribution of the cation-exchange and chelation mechanisms to the retention of probe transition metal ions ( $Cd^{2+}$ ,  $Cu^{2+}$ ,  $Zn^{2+}$ ) has been elucidated, observing that  $Cd^{2+}$  is retained mainly by cation-exchange mechanism, whereas chelation is mainly responsible for  $Cu^{2+}$  and  $Zn^{2+}$  retention.

The chelating properties revealed for the ED3A-MCM41 have been exploited for the determination of the above mentioned metal ions in a highly saline matrix of environmental interest.

## Acknowledgements

The financial contribution from Piedmont Region, Italy (Scientific and Applied Research Project E28) and from MIUR (Ministero dell'Istruzione, dell'Università e della Ricerca, Italy) PRIN 2008 (Hierarchical Porosity Materials for gas adsorption and pollutants removal) are gratefully acknowledged.

## REFERENCES

- 1 M.H. Lim and A. Stein, *Chem. Mater.* 1999, **11**, 3285-3295.
- 2 M.C. Bruzzoniti, A. Prella, C. Sarzanini, B. Onida, S. Fiorilli, E. Garrone, *J. Sep. Sci.*, 2007, **30**, 2414-2420.
- 3 M.C. Bruzzoniti, R.M. De Carlo, S. Fiorilli, B. Onida, C. Sarzanini, *J. Chromatogr. A*, 2009, **1216**, 5540–5547.
- 4 M. R. Jamali, Y. Assadi, F. Shemirani, M. Salavati-Niasari, *Talanta*, 2007, **71**, 1524-529.
- 5 M. R. Jamali, Y. Assadi, F. Shemirani, M. R. Milani Hosseini, R. R. Kozani, M. Masteri-Farahani, M. Salavati-Niasari, *Anal. Chim. Acta*, 2006, **579**, 68-73.
- 6 D.-H. Lin, Y.-X. Jiang, Y. Wang and S.-G. Sun, *J. of Nanom.*, 2008, doi:10.1155/2008/473791
- 7 V. Ganesan, A. Walcarius, *Langmuir* 2004, **20**, 3632-3640.
- 8 S. A. Trammell, M. Zeinali, B. J. Melde, P. T. Charles, F. L. Velez, M. A. Dinderman, A. Kusterbeck, and M. A. Markowitz, *Anal. Chem.*, 2008, **80**, 4627-4633.
- 9 S. Inagaki, S. Guan, Q. Yang, M. P. Kapoor and T. Shimada, *Chem. Comm.*, 2008, 202-204.
- 10 H. Grajeka, J. Paciura-Zadroz, Z. Witkiewicza, *J. Chromatogr. A*, 2008, **1194**, 118–127.
- 11 M. Anbia, N. Mohammadi, K. Mohammadi, *J. Hazard. Mater.*, 2010, **176**, 965–972
- 12 K.A. Northcott, K. Miyakawa, S. Oshima, Y. Komatsu, J.M. Perera, G.W. Stevens, *Chem. Eng. J.*, 2010, **157**, 25–28.
- 13 H. Sepehrian, S.J. Ahmadi, S. Waqif-Husain, H. Faghihian, H. Alighanbari, *J. Hazard. Mater.*, 2010, **176**, 252–256.
- 14 K.F. Lam, C.M. Fong, K.L. Yeung, G. McKay, *Chem. Eng. J.*, 2008, **145**, 185–195.
- 15 T. Yasmina, K. Müller, *J. Chromatogr. A*, 2010, **1217**, 3362–3374.
- 16 T. Martin, A. Galarneau, F. Di Renzo, D. Brunel, F. Fajula *Chem. Mater.* **2004**, *16*, 1725-1731.17 L. Yang, Y. Wang, G. Luo, Y. Dai, *Particuology*, 2008, **6**, 143-148.
- 18 H. Zhonga, G. Zhua, P.Wanga, J. Liua, J. Yanga, Q. Yanga, *J. Chromatogr. A*, 2008, **1190**, 232–240.
- 19 J. Wanga, L. Huang, M. Xue, L. Liu, Y. Wanga, L. Gao, J. Zhu, Z. Zou, *Appl. Surf. Sci.*, 2008, **254**, 5329-5335.
- 20 Y. Li, S. Cheng, P. Dai, X. Liang and Y. Ke, *Chem. Comm.*, 2009, 1085-1087.
- 21 M.A. Markowitz, J. Klaehn, R.A. Hendel, S.B. Qadriq, S.L. Golledge, D.G. Castner, B.P. Gaber, *J. Phys. Chem. B* 2000, **104**, 10820-10826.
- 22 C. Yang, B. Zibrowius, F. Schüth, *Chem. Comm.* 2003, **14**, 1772-1773
- 23 K. Takei, R. Takahashi and T. Noguch, *J. Phys. Chem. B*, 2008, **112**, 6725-6731.
- 24 G. Socrates, “*Infrared and Raman Characteristic Group Frequencies. Tables and Charts*”, Third Edition, John Wiley & Sons, 2001, pag 127.
- 25 S. Fiorilli, B. Onida, B. Bonelli and E. Garrone, *J. Phys. Chem. B*, 2005, **109**, 16725-16729
- 26 S. Badilescu, C. Sandorfy, *Can. J. Chem.*, 1987, **65**, 924-927
- 27 J.S. Fritz, D.T. Gjerde, *Ion Chromatography* Wiley-VCH 2009 Weinheim
- 28 H. Small, in “*Ion Chromatography*”, Plenum Press, New York, 1989
- 29 P. Jones, P.N. Nesterenko, *J. Chromatogr. A*, 1997, **789**, 413-435
- 30 W. Bashir, E. Tyrrell, O. Feeney, B. Paull, *J. Chromatogr. A*, 2002, **964**, 113-122.
- 31 L.G. Sillen, A.E. Martell, *Stability Constants Special Publication No. 17* . London. The Chemical Society 1964
- 32 CRC Handbook of Organic Analytical Reagents, K. L. Cheng, K. Ueno, T. Imamura eds., CRC Press, Boca Raton 1982

**Table 1.** Formation constants for the metal ions studied.<sup>31</sup>

	<b>Ligand</b>		
	<b>HEDTA<sup>a)</sup></b>	<b>PDCA</b>	<b>Oxalic acid</b>
	<b>logK<sub>ML</sub></b>	<b>logK<sub>ML2</sub></b>	<b>logK<sub>ML2</sub></b>
Cd <sup>2+</sup>	13.6	11.2	4.7
Cu <sup>2+</sup>	17.6	16.5	10.5
Zn <sup>2+</sup>	14.5	11.9	7.6

<sup>a)</sup> The chelating moiety of the ED3A-MCM41 phase was assimilated to the N-(2-Hydroxyethyl)ethylenediamine-N, N', N'-triacetic acid (HEDTA). The pKa values are 2.51, 5.31, 9.86 for pK<sub>1</sub>, pK<sub>2</sub> and pK<sub>3</sub>, respectively.<sup>32</sup>

**Table 2.** Retention results for the metal ions studied at different mobile phase compositions.

<b>Eluent</b>	<b>k</b>		
	<b>Cd<sup>2+</sup></b>	<b>Cu<sup>2+</sup></b>	<b>Zn<sup>2+</sup></b>
1 mM oxalic acid, pH 2.9	<i>n.e.</i>	<i>n.e.</i>	<i>n.e.</i>
5 mM oxalic acid, pH 2.4	2.5	<i>n.e.</i>	24.1
20 Mm oxalic acid, pH 1.8	0.04	13.5	1.4
15 mM MSA, pH 1.8	0.3	<i>n.e.<sup>a)</sup></i>	<i>n.e.<sup>a)</sup></i>
20 mM oxalic acid, pH 4.0 by addition of NaOH	<i>n.e.</i>	<i>n.e.</i>	<i>n.e.</i>

*n.e.* not eluted within 100 min

<sup>a)</sup> see §3.1.1 and Figure 7



## Figure captions

**Figure 1.** Scheme of ED3A-MCM41.

**Figure 2.** X-Ray diffraction of extracted ED3A-MCM41 sample

**Figure 3.** Nitrogen adsorption-desorption isotherm of extracted ED3A-MCM41 sample.

**Figure 4.** IR spectrum of extracted ED3A-MCM41 after outgassing at room temperature. Inset: detail of the low frequencies region.

**Figure 5.** IR spectra of ED3A-MCM41 after outgassing at room temperature (solid curve) and at 100 °C (broken curve).

**Figure 6.** IR spectra of ED3A-MCM41 after outgassing at 150 °C (curve 1) and in contact with NH<sub>3</sub> at increasing equilibrium pressure (0.01 – 150 mbar). Arrows indicate the change in band intensity upon increasing NH<sub>3</sub> pressure.

**Figure 7.** Effect of methanesulfonic acid in the eluent on the k of Cd<sup>2+</sup>, Zn<sup>2+</sup> and Cu<sup>2+</sup> not eluted. Column: ED3A-MCM41.

**Figure 8.** Effect of ionic strength on the k of Cd<sup>2+</sup>, Zn<sup>2+</sup> and Cu<sup>2+</sup> not eluted. Column: ED3A-MCM41. Eluent: 3.5 mM MSA, NaNO<sub>3</sub> as shown.

**Figure 9.** Effect of PDCA concentration in the eluent (pH 2 by HNO<sub>3</sub>) on the retention behaviour of Cd<sup>2+</sup>, Cu<sup>2+</sup> and Zn<sup>2+</sup> on the ED3A-MCM41 column. Inset: overlay of chromatograms obtained at 2.5 mM PDCA, pH 2.

**Figure 10.** Effect of pH on retention factors of metal ions. Eluent: 2.5 mM PDCA, pH as shown. Inset: schematic representation of the main mechanisms involved as a function of eluent pH.

**Figure 11a.** Separation of Cd<sup>2+</sup>, Zn<sup>2+</sup> and Cu<sup>2+</sup>. Eluent: 2.5 mM PDCA, 20 mM oxalic acid, pH 1.8.

**Figure 11b.** Optimized separation of Cd<sup>2+</sup>, Zn<sup>2+</sup> and Cu<sup>2+</sup>. Eluent: gradient 0-3 min: 20 mM Oxalic acid, 50 mM NaNO<sub>3</sub>, pH 1.8; 3.1 min: step change to 2.5 mM PDCA, 50 mM NaNO<sub>3</sub>, pH 2.8.

**Figure 12.** Analysis of the metal ions studied in synthetic seawater (0.5 M NaCl) by ED3A-MCM41 column with the optimized gradient (see Figure 6b). (a): 0.5 M NaCl; (b): 2.5 ppm Cd<sup>2+</sup>, Zn<sup>2+</sup> and Cu<sup>2+</sup> in 0.5 M NaCl.

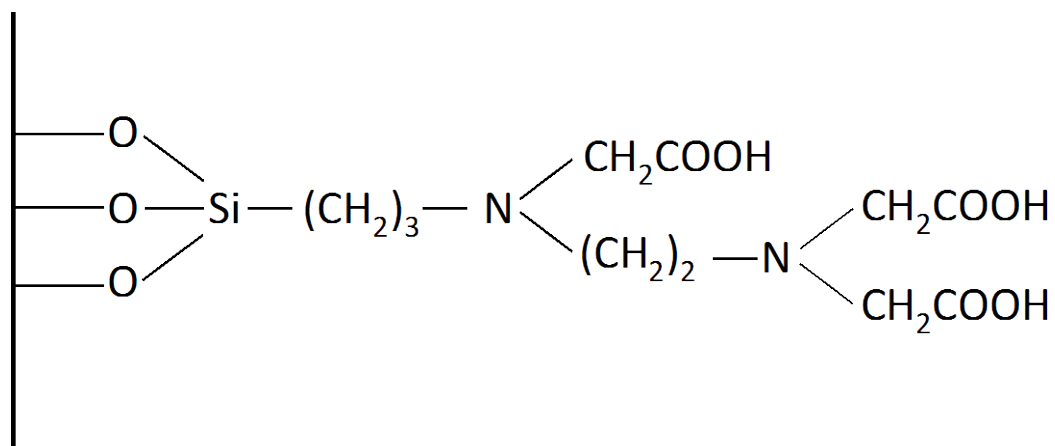


**Figure 1.** Scheme of ED3A-MCM41.

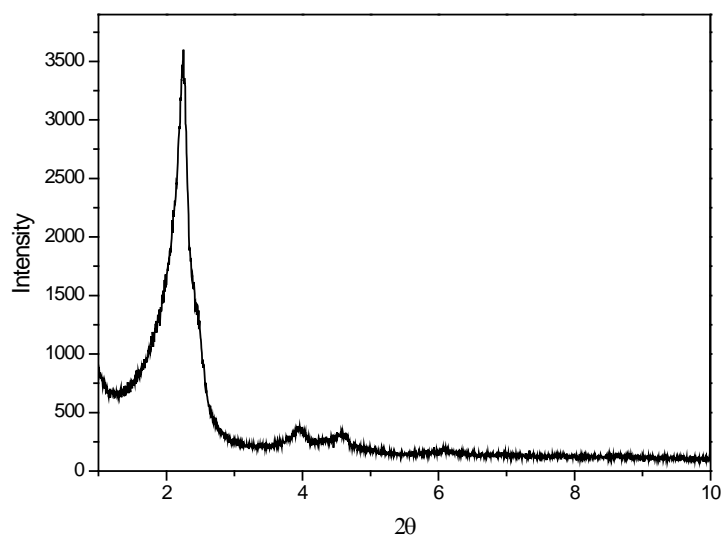


**Figure 2.** X-Ray diffraction of extracted ED3A-MCM41 sample

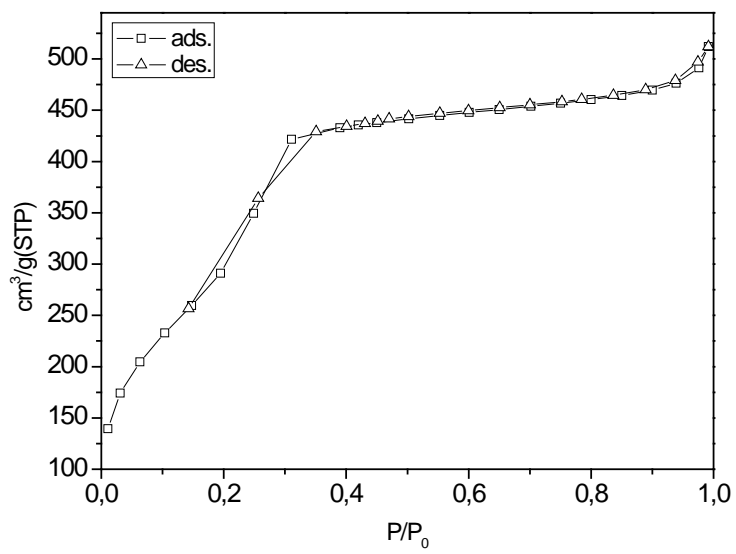


**Figure 3.** Nitrogen adsorption-desorption isotherm of extracted ED3A-MCM41 sample.

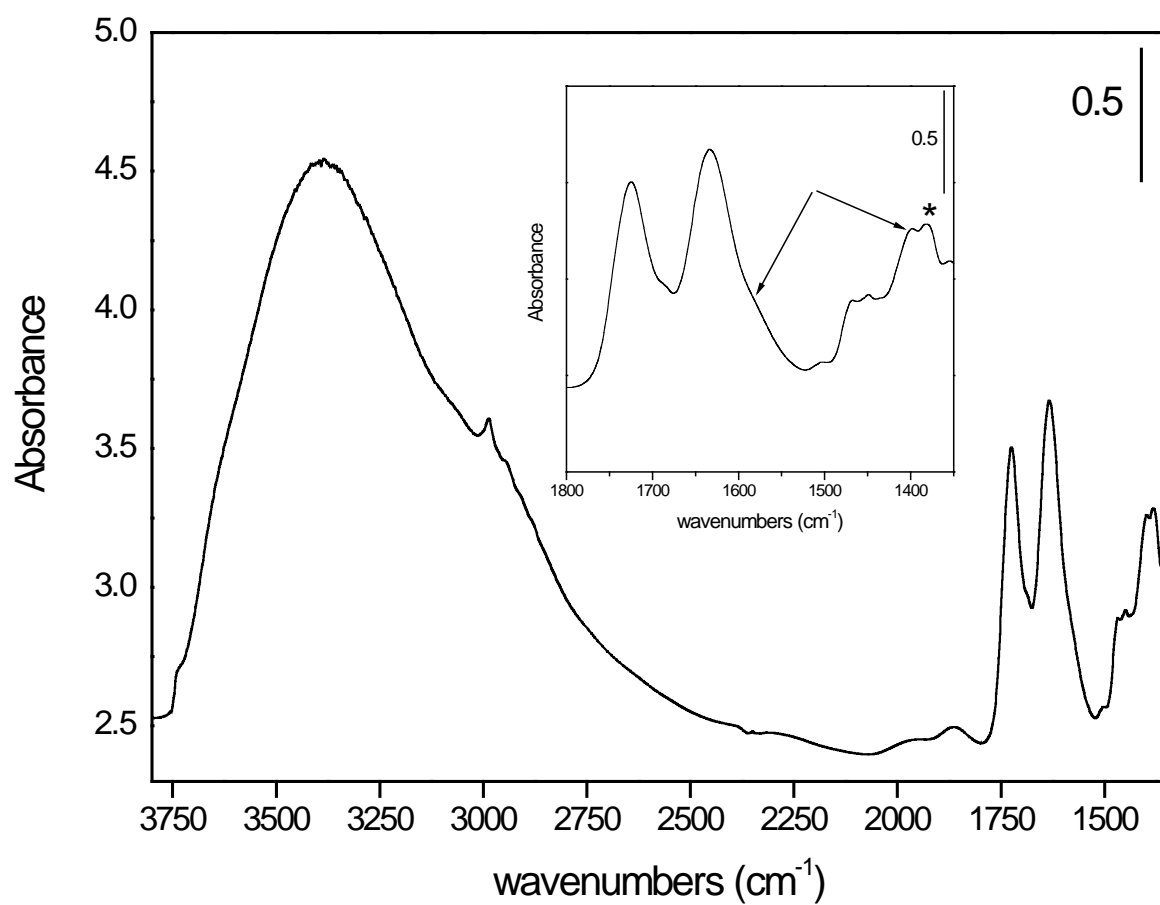


**Figure 4.** IR spectrum of extracted ED3A-MCM41 after outgassing at room temperature. Inset: detail of the low frequencies region.

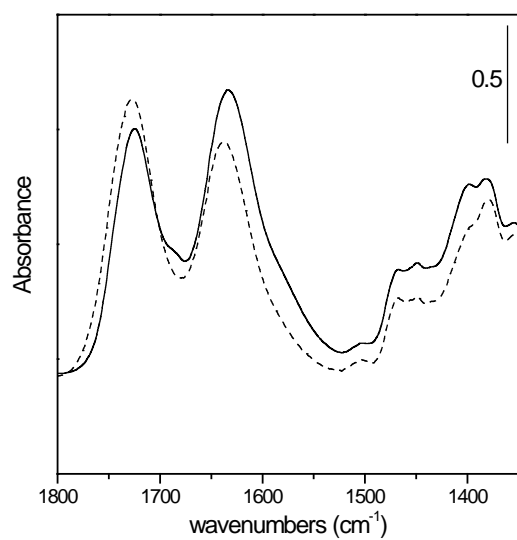


**Figure 5.** IR spectra of ED3A-MCM41 after outgassing at room temperature (solid curve) and at 100 °C (broken curve).

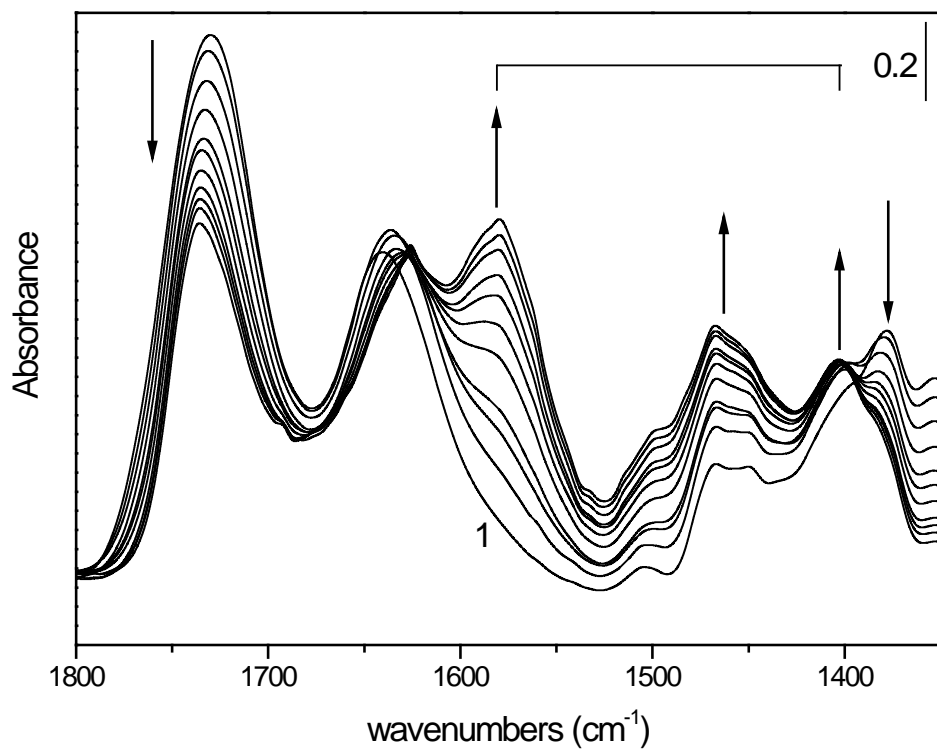


**Figure 6.** IR spectra of ED3A-MCM41 after outgassing at 150 °C (curve 1) and in contact with NH<sub>3</sub> at increasing equilibrium pressure (0.01 – 150 mbar). Arrows indicate the change in band intensity upon increasing NH<sub>3</sub> pressure.

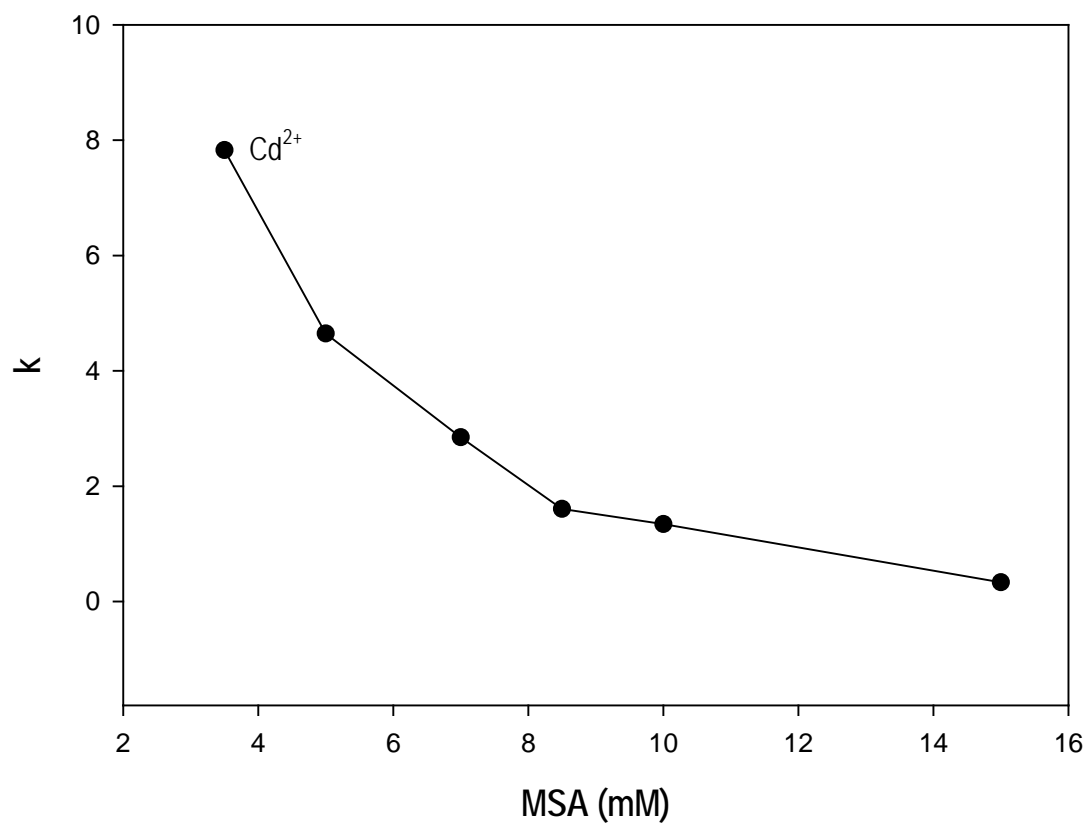


**Figure 7.** Effect of methanesulfonic acid in the eluent on the  $k$  of  $\text{Cd}^{2+}$ ,  $\text{Zn}^{2+}$  and  $\text{Cu}^{2+}$  not eluted. Column: ED3A-MCM41.

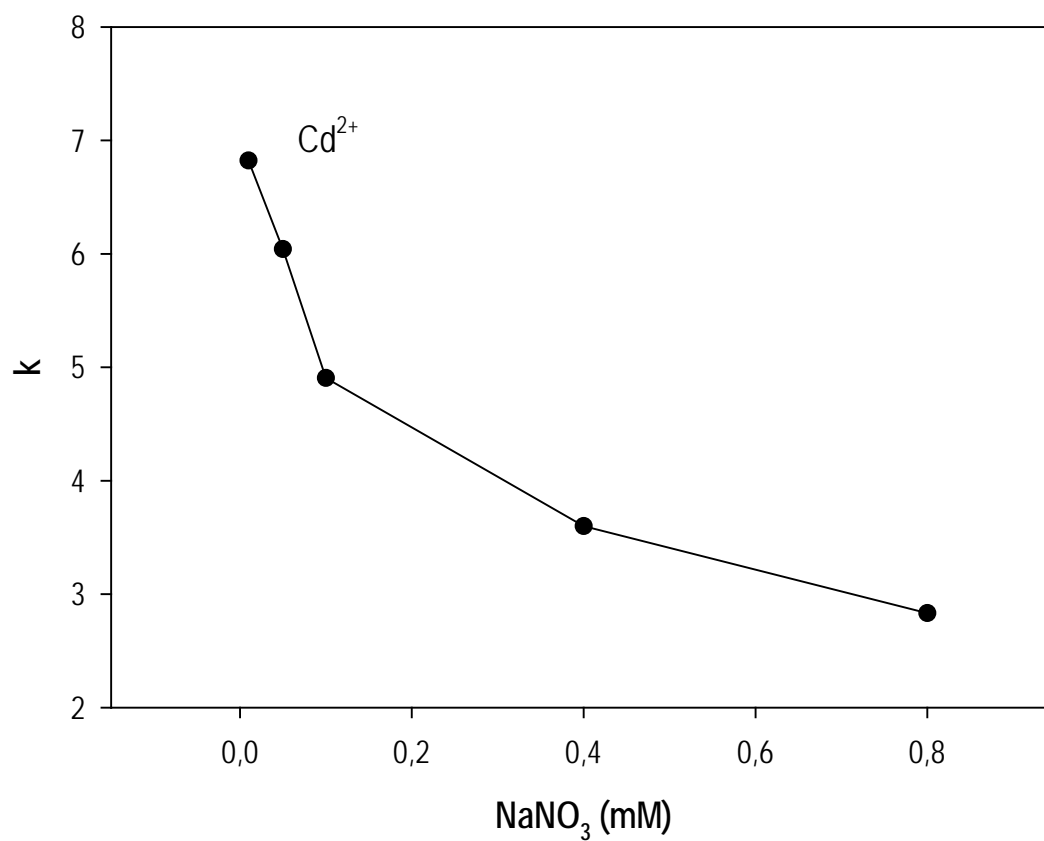


**Figure 8.** Effect of ionic strength on the k of Cd<sup>2+</sup>. Zn<sup>2+</sup> and Cu<sup>2+</sup> not eluted. Column: ED3A-MCM41. Eluent: 3.5 mM MSA, NaNO<sub>3</sub> as shown.



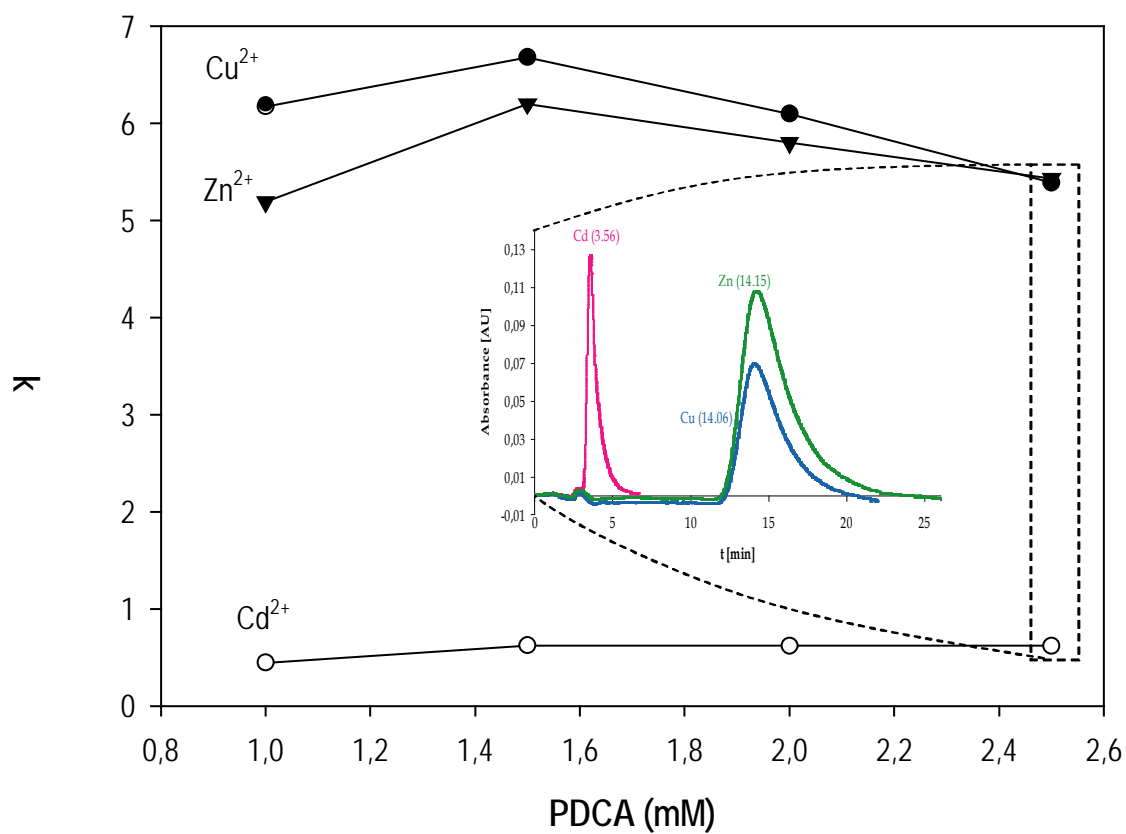


**Figure 9.** Effect of PDCA concentration in the eluent (pH 2 by  $\text{HNO}_3$ ) on the retention behaviour of  $\text{Cd}^{2+}$ ,  $\text{Cu}^{2+}$  and  $\text{Zn}^{2+}$  on the ED3A-MCM41 column. Inset: overlay of chromatograms obtained at 2.5 mM PDCA, pH 2.

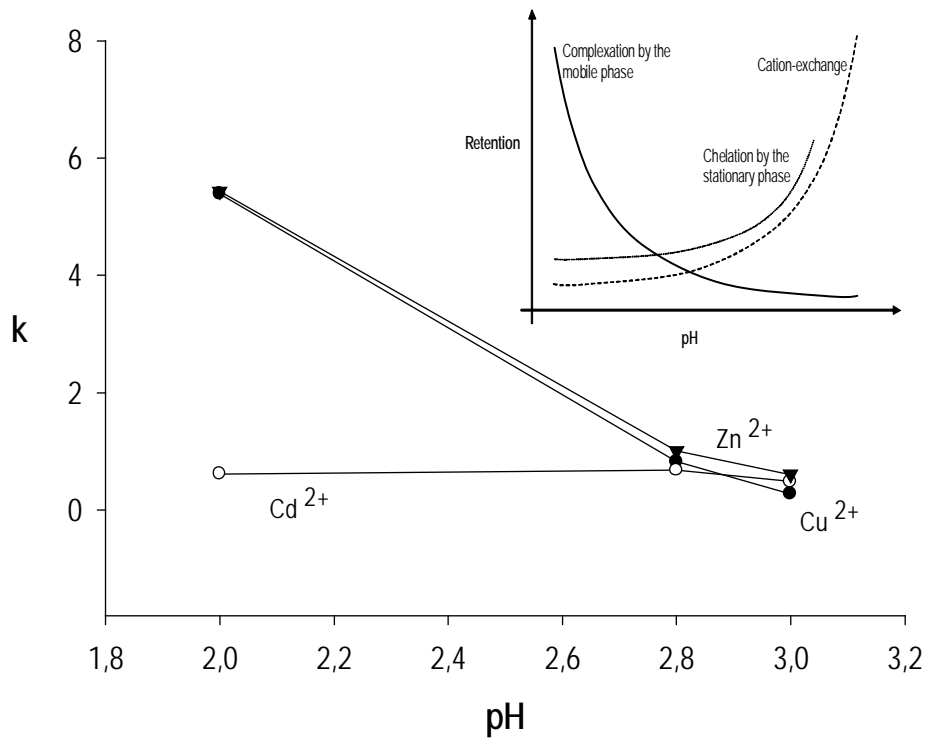


**Figure 10.** Effect of pH on retention factors of metal ions. Eluent: 2.5 mM PDCA, pH as shown. Inset: schematic representation of the main mechanisms involved as a function of eluent pH.

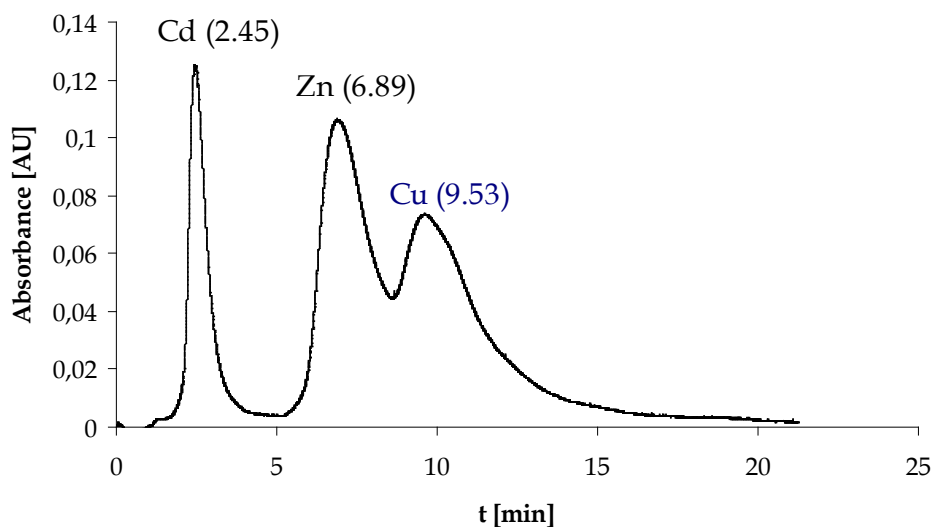


**Figure 11a.** Separation of  $\text{Cd}^{2+}$ ,  $\text{Zn}^{2+}$  and  $\text{Cu}^{2+}$ . Eluent: 2.5 mM PDCA, 20 mM oxalic acid, pH 1.8.

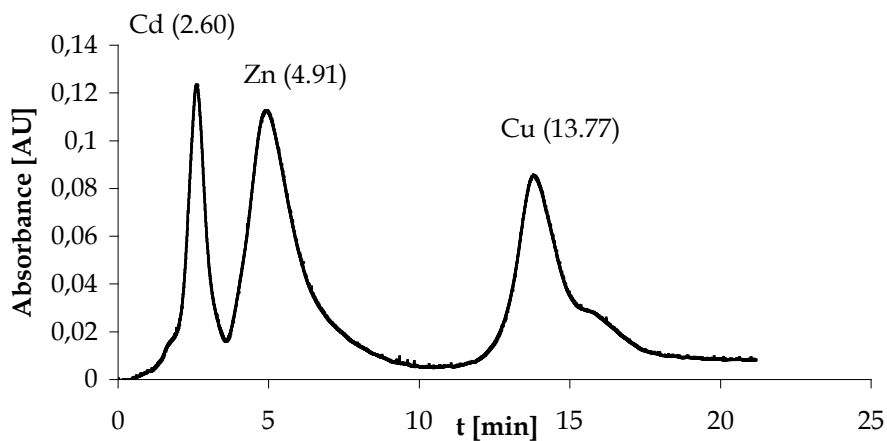


**Figure 11b.** Optimized separation of  $\text{Cd}^{2+}$ ,  $\text{Zn}^{2+}$  and  $\text{Cu}^{2+}$ . Eluent: gradient 0-3 min: 20 mM Oxalic acid, 50 mM  $\text{NaNO}_3$ , pH 1.8; 3.1 min: step change to 2.5 mM PDCA, 50 mM  $\text{NaNO}_3$ , pH 2.8.

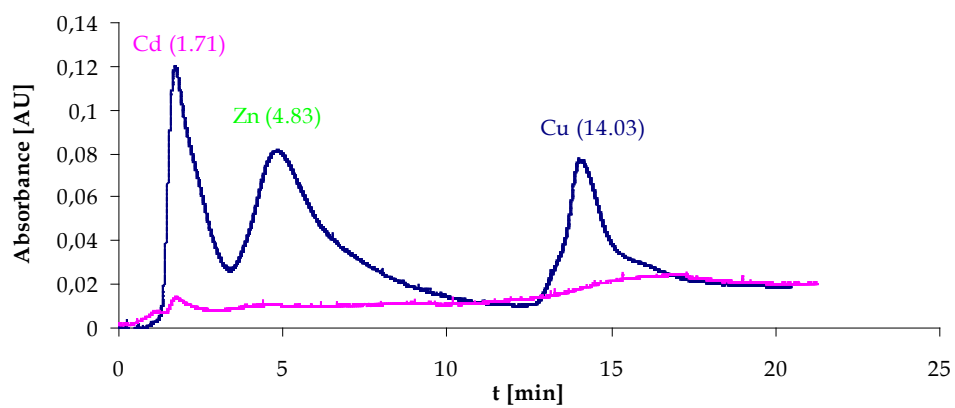


**Figure 12.** Analysis of the metal ions studied in synthetic seawater (0.5 M NaCl) by ED3A-MCM41 column with the optimized gradient (see Figure 6b). (a): 0.5 M NaCl; (b): 2.5 ppm Cd<sup>2+</sup>, Zn<sup>2+</sup> and Cu<sup>2+</sup> in 0.5 M NaCl.

## Supplementary Information

### Scanning Electron Microscopy (SEM)

SEM micrograph of ED3A-MCM41 (FEI QUANTA INSPECT 200 LV) shows spherical particles having size smaller than 1  $\mu\text{m}$ .

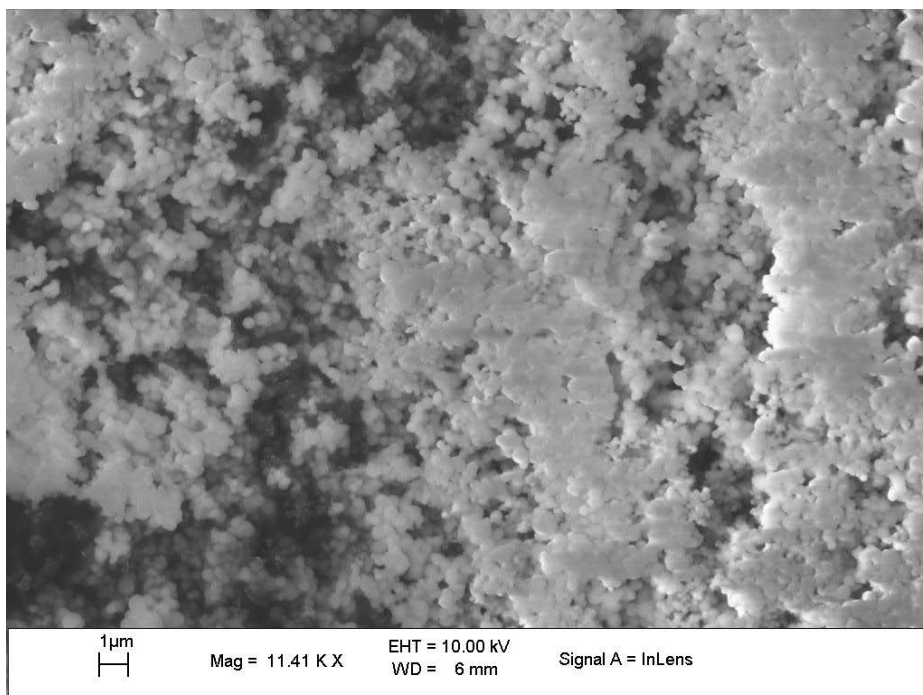


Fig S1 Scanning Electron Microscopy image of ED3A-MCM41